

Nanodielectric mapping of a model polystyrene-poly(vinyl acetate) blend by electrostatic force microscopy

C. Riedel,^{1,2,3} R. Arinero,¹ Ph. Tordjeman,^{4,*} G. L ev eque,¹ G. A. Schwartz,⁵ A. Alegria,^{5,3} and J. Colmenero^{5,2,3}

¹*Institut d'Electronique du Sud (IES), UMR CNRS 5214, Universit  Montpellier II, CC 082, Place E. Bataillon, 34095 Montpellier Cedex, France*

²*Donostia International Physics Center, Paseo Manuel de Lardizabal 4, 20018 San Sebasti n, Spain*

³*Departamento de F sica de Materiales, Facultad de Qu mica, UPV/EHU, Apartado 1072, 20080 San Sebasti n, Spain*

⁴*Institut de M canique des fluides (IMFT), INPT-CNRS, Universit  de Toulouse, 1 All e du Professeur Camille Soula, 31400 Toulouse, France*

⁵*Centro de F sica de Materiales CSIC-UPV/EHU, Edificio Korta, 20018 San Sebasti n, Spain*

(Received 10 September 2009; revised manuscript received 6 November 2009; published 8 January 2010)

We present a simple method to quantitatively image the dielectric permittivity of soft materials at nanoscale using electrostatic force microscopy (EFM) by means of the double pass method. The EFM experiments are based on the measurement of the frequency shifts of the oscillating tip biased at two different voltages. A numerical treatment based on the equivalent charge method allows extracting the values of the dielectric permittivity at each image point. This method can be applied with no restrictions of film thickness and tip radius. This method has been applied to image the morphology and the nanodielectric properties of a model polymer blend of polystyrene and poly(vinyl acetate).

DOI: [10.1103/PhysRevE.81.010801](https://doi.org/10.1103/PhysRevE.81.010801)

PACS number(s): 61.41.+e, 62.23.-c

Nanostructured polymers, nanoparticle composites, and biological membranes are typical complex systems for which local properties, local structure, and composition determine the properties and the functionality on the microscale and macroscale. Understanding the behavior of these complex systems is based on the parallel studies of the local structure or composition and of the local properties. For electronic materials, scanning tunneling microscopy is the appropriate technique to realize such studies. For soft matter, atomic force microscopy (AFM) [1] can be used but requires the development of new experiments and procedures to measure quantitatively the properties at local scale. In this Rapid Communication, we show that the morphology and the dielectric properties of a model polymer blend can be measured at the nanoscale by coupling electrostatic force microscopy (EFM)-AFM experiments with numerical simulations based on the equivalent charge method (ECM).[2,3]

In the last five years, the quantitative analysis of the dielectric permittivity at nanoscale has become a great challenge. Kravtsov *et al.* [4,5] have been the first to present a quantitative value of the dielectric constant of a polymer at the nanoscale using phase shift images obtained by the double pass method. However, the quantification is only possible when the tip radius is negligible compared to the thickness of the polymer and is therefore not suitable for the study of ultrathin polymer films or biological membranes. Moreover, the dielectric constants of two reference polymers are required to measure a third unknown one. Using the so-called nanoscale dielectric microscopy, Fumagalli *et al.* [6] have been able to quantify and image the low-frequency dielectric constant of a single biomembrane. Using a tip with a nominal radius of 100–200 nm they estimate the spatial lateral resolution around ~ 70 nm. The experiment is based on

the measurement of the local capacitance by a fully customized current amplifier and lock-in board integrated with the AFM electronics [7,8] that allows capacitance measurements with attofarad resolution. [9] Following another approach based on force detection by AFM experiments, other authors have characterized the dielectric properties of carbon nanotubes and biomembranes. [10,11] Recently, Crider *et al.* [12,13] have used ultrahigh vacuum atomic force microscopy in order to characterize the complex dielectric permittivity [$\epsilon^*(\omega) = \epsilon' - i\epsilon''$] of poly(vinyl acetate) (PVAc) polymer. This experiment was realized by applying an ac bias voltage of variable frequency (ω). From the in and quadrature phase components of the sensor signal response and using a phenomenological model, they obtained the qualitative frequency dependence of ϵ' and ϵ'' .

In order to determine quantitatively the relative dielectric constant ϵ_r of soft materials at the nanoscale, we have developed an EFM method based on the measurement of an electric force gradient $\text{grad}_{DC} F$ while applying a V_{DC} voltage between a tip and a sample holder on which a thin film of a soft material is deposited. The force gradient is related to the cantilever-tip-sample capacitance $C(z)$ by $\text{grad}_{DC} F = \frac{1}{2}[\partial^2 C(z)/\partial z^2]V_{DC}^2$, where z is the tip-sample distance. $C(z)$ is a sum of the tip apex capacitance $C_{apex}(z)$ and the stray capacitance $C_{stray}(z)$, associated with the tip cone and the cantilever contributions. According to Fumagalli *et al.* [7], for nanometric displacements around the measuring position, $C_{stray}(z)$ varies linearly with the distance and, thus, can be neglected in the calculation of the second derivative $\partial^2 C(z)/\partial z^2$. The local electrostatic force gradient is a function of the resonance frequency shift Δf_0 , which can be measured by keeping the phase shift constant: $\Delta f_0/f_0 \cong -\frac{1}{2}[(\text{grad}_{DC} F)/k_c]$, [14] where k_c is the stiffness of the cantilever. As expected from previous relations, the curves $\Delta f_0(V_{DC})$ have the parabolic form, $-a_{\Delta f_0}(z)V_{DC}^2$, where $a_{\Delta f_0}(z)$ is related to the tip-sample capacitance by the

*Corresponding author; philippe.tordjeman@imft.fr

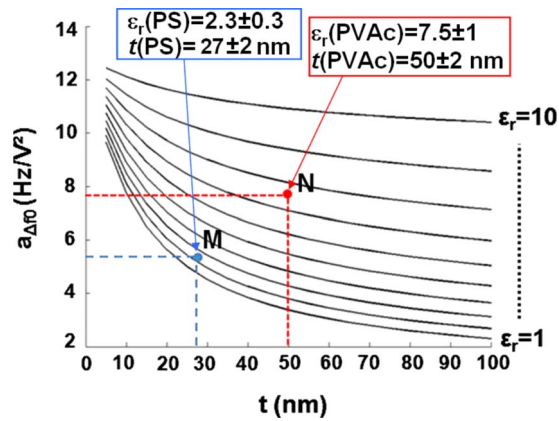


FIG. 1. (Color online) Numerical simulations based on ECM of the curves $a_{\Delta f_0}(t, \epsilon_r)$, where t is the sample thickness and ϵ_r is the relative dielectric permittivity, for a tip radius $R=19$ nm and a tip-sample distance $z_0=18$ nm. $M(t, a_{\Delta f_0})$ and $N(t, a_{\Delta f_0})$ are typical points obtained from AFM topography and EFM images (Fig. 3), respectively, on the PS matrix and the PVAc nodules of the studied polymer blend thin film. ϵ_r can be deduced by interpolating these points with simulated curves.

expressions $a_{\Delta f_0}(z) = (f_0/4k_c)[\partial^2 C(z)/\partial z^2]$. EFM experiments were realized following the double pass method [14–16]: during a first scan the sample topography is acquired in the amplitude-controlled mode (Tapping®). Then, the tip is retracted by a constant height (“lift height”) and the amplitude of the tip vibration is reduced to stay in the linear regime of the tip-sample interactions. A second scan allows us to measure the frequency shift Δf_0 produced by a constant tip potential V_{DC} , and $a_{\Delta f_0}(z)$ is extracted from the curves $\Delta f_0(V_{DC})$. At this stage, we used numerical simulations to calculate the ϵ_r value of the sample in the frame of ECM [2,3]. For a tip-sample geometry, a discrete distribution of free and image charges is modeled such that they create a potential V_0 in the air and V_1 in the dielectric, satisfying the appropriate boundary conditions at the tip surface, air/sample interface, and sample/substrate interface. Only the paraboloidal tip extremity (~ 1 μm) is considered in the calculations. A good representation can be given by approximately ten charges for the cone and four charges for the tip, as mentioned in [17]. The numerical simulations show that the tip angle is not a very sensitive parameter. In this work, we used the value given by the manufacturer, $\theta=15^\circ$. The tip radius R is the main geometrical parameter and is determined using the protocol previously reported. [17] Once the position and the value of the charges and image charges are known, it is possible to calculate the tip-sample force, the force gradient $\text{grad}_{DC} F$, and finally the coefficient $a_{\Delta f_0}(z)$ as a function of R , the thickness of the film t , and the dielectric constant ϵ_r (Fig. 1). Using this calculation, the measured values of $a_{\Delta f_0}(z)$ can be mapped onto actual local permittivity values. The advantage of ECM is that it allows working without any restriction on the thickness of the sample and the radius of the tip. In addition, the high sensitivity of EFM to detect electrostatic force gradients permits us to work with sharp tips with radius as low as 20 nm, giving an excellent lateral resolution.

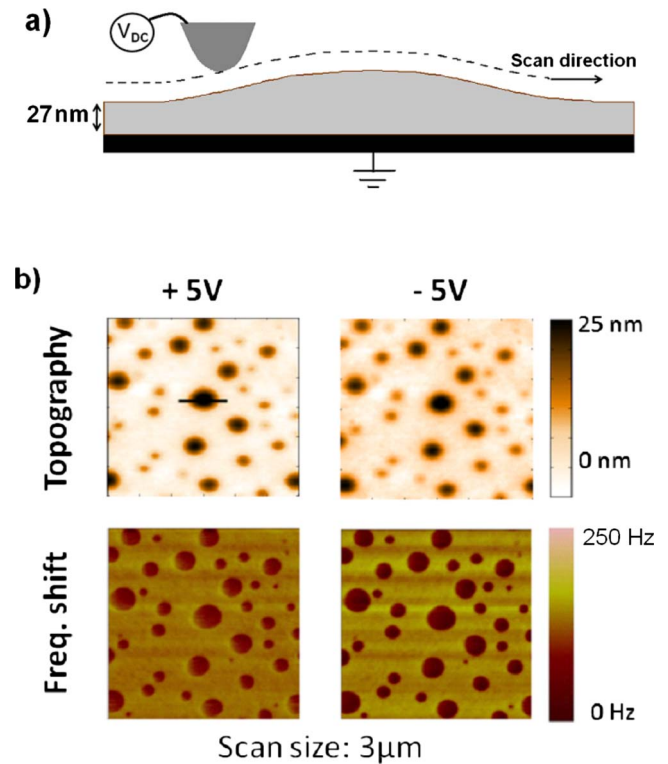


FIG. 2. (Color online) (a) Typical topographic profile of PVAc islands in a PS matrix. Both tip and polymer film are represented at the same scale. The dash line represents the tip motion during the second scan. (b) Topography and frequency shift measured by the double pass method at +5 and -5 V on the PVAc/PS films. The black line corresponds to the profile appearing in (a).

Following this procedure, we have studied at the nanoscale the morphology and the dielectric properties of a model nanostructured soft material constituted by an immiscible blend of polystyrene (PS) and of PVAc (PS: $M_n=66\,900$ g/mol and $M_w=71\,000$ g/mol; PVAc: $M_n=33\,200$ g/mol and $M_w=93\,100$ g/mol). The sample film was prepared from a solution of the polymers (1% w/w in toluene with 75% PS w/w and 25% w/w PVAc). The volume fraction of PVAc is $\Phi=16.4\%$. The solution was subsequently spin coated [18] on a conductive gold substrate at 3000 rpm. The film exhibits a nodular morphology of PVAc in a continuum phase of PS [Fig. 2(b)]. The nodules of PVAc have a mean height measured by AFM around 50 nm and the PS has a homogeneous thickness of around 27 nm. The dielectric behavior of these polymers has been previously characterized in the literature [19–22]. At room temperature both polymers present similar dielectric permittivity, but they are substantially different above 50 $^\circ\text{C}$ providing a good dielectric contrast.

EFM experiments were therefore realized at 70 $^\circ\text{C}$ with a Veeco Enviroscope™ equipped with a Lakeshore temperature controller. We have used a standard Pt-Ir coated tip (Nanosensors EFM). The cantilever free resonance frequency was $f_0=70.13$ kHz and the stiffness $k_c=4.5$ N m $^{-1}$ was calculated by the thermal tune method. [23] The tip radius was $R=19 \pm 2$ nm. In order to preserve the tip from wear, all the experiments were carried out in a very soft

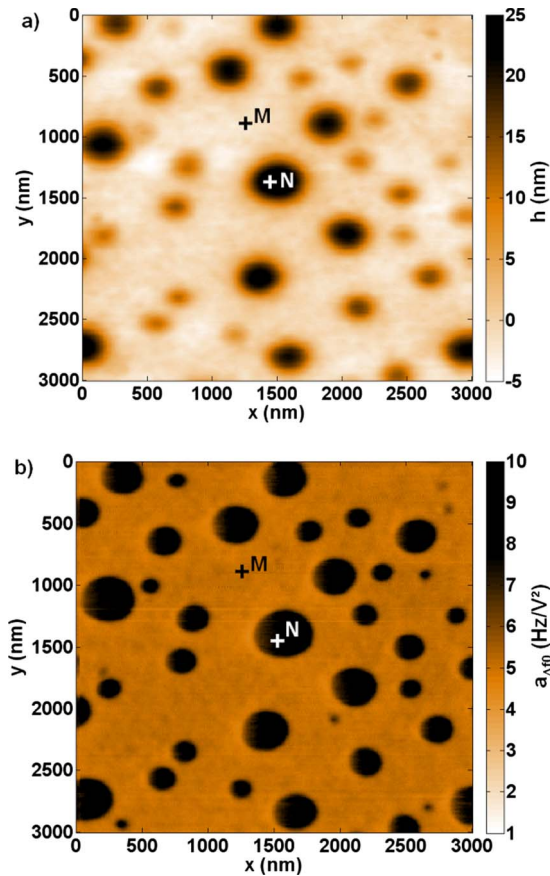


FIG. 3. (Color online) (a) Topography of the PVAc/PS film. (b) Corresponding map of the coefficient $a_{\Delta f_0}$. Values of t and $a_{\Delta f_0}$ at points M (PS matrix) and N (PVAc nodule) have been reported in Fig. 1 where they have been interpolated with ECM simulated curves in order to extract the corresponding value of ϵ_r .

tapping mode. When recording the topography signal, during the first scan, the tip was carefully maintained in a light attractive regime (negative mechanical phase shift of the cantilever oscillation). We checked that after several series of measurements the tip radius did not increase significantly, as expected for EFM polymer characterization.

Frequency shifts were measured by means of the succession of two double pass scans at a fixed value of the tip-sample distance, $z_0 = 18 \pm 2$ nm, and applying two different voltages of +5 and -5 V (Fig. 2). When the surface is characterized by a zero potential, only a single double pass scan is necessary to implement our method. However, we recommend doing two double pass scans in order to verify the good accuracy of the measurements and to check the symmetry of the parabola with respect to the 0 V axis. We note that the applied dc voltage can influence the bending of the cantilever and hence can induce notable variations of the tip-sample distance. In our experiments, we estimate a 2 nN maximum force acting on the cantilever, giving a precision of the tip-sample distance of $\sim 2\%$. This value is low compared with the 10% error in z determined from amplitude-distance curves. In the present study, due to the absence of free charges, the frequency shift at a zero voltage is found to be nearly null in the scanned area. In order to ensure that the

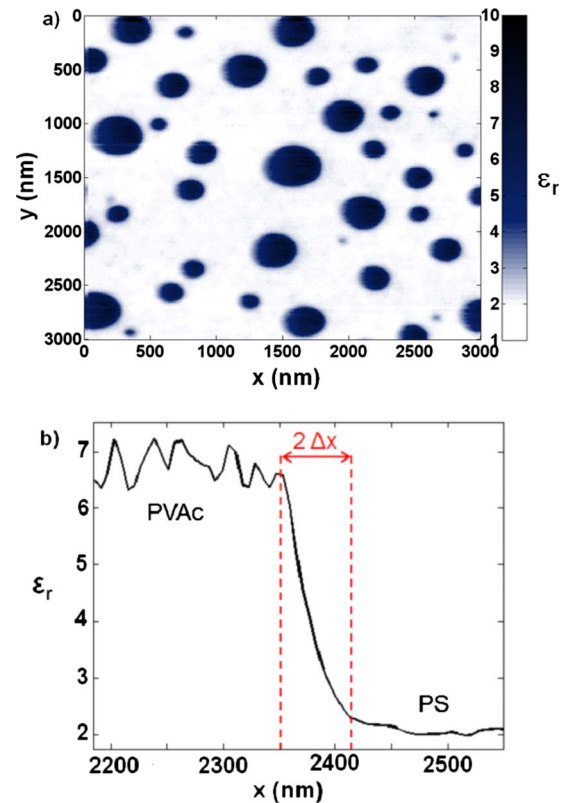


FIG. 4. (Color online) (a) Map of the dielectric constant of the PVAc/PS film obtained by processing images shown in Fig. 3. (b) Typical profile of the dielectric permittivity across the PVAc/PS interface.

two frequency shifts correspond to the same sample point, the topography of the two images at different biases should be as similar as possible [Fig. 2(b)]. However, working at 70°C a non-negligible drift is observed. Translation effects have been numerically corrected by the introduction of a correlation function. Note that, as the height is an important parameter to calculate ϵ_r , images have to be properly flattened using only the topography information from the PS matrix. Using these two measurements and assuming a zero-frequency shift for a zero voltage applied, we can calculate the coefficient $a_{\Delta f_0}$ at each point of the topographic image. Figures 3(a) and 3(b) present the topography and the corresponding map of the coefficient $a_{\Delta f_0}$, respectively. In the general case, in order to take into account the nonzero contact potential V_{CP} , a third image has to be recorded at another applied voltage (for example, at 0 V). A map of the parabolic coefficient $a_{\Delta f_0}$ could be obtained from frequency shift images using the equation $\Delta f = a_{\Delta f_0}(V_{DC} - V_{CP})^2$.

From EFM results and ECM numerical simulations [$a_{\Delta f_0}(t, \epsilon_r)$ curves], we calculated ϵ_r in each point of the image (the sample thickness t was determined by AFM, measuring the height difference between the polymer surface and the gold substrate after the films were cut using a sharp steel knife). As an example, points M (PS) and N (PVAc) in Figs. 1 and 3 are characterized by $t(\text{M}) = 27 \pm 2$ nm, $a_{\Delta f_0}(\text{M}) = 5.2 \pm 0.3$ Hz/V² and $t(\text{N}) = 50 \pm 2$ nm, $a_{\Delta f_0}(\text{N}) = 7.8 \pm 0.7$ Hz/V², respectively. After successive interpola-

tions between different $a_{\Delta f_0}(t, \epsilon_r)$ curves, we found $\epsilon_r = 2.3 \pm 0.3$ for PS and $\epsilon_r = 7.5 \pm 1$ for PVAc, values in agreement with the literature [19–22].

Figure 4(a) shows a quantitative map of the dielectric constant of the PVAc/PS film at the nanoscale. The small asymmetry observed on the islands of PVAc (on the x axis) is most likely attributed to the scanning process (only retrace signal was recorded). We estimate an upper limit of the spatial resolution Δx around ~ 30 nm, which corresponds to half the distance necessary to achieve the transition between the dielectric level of the island of PVAc and the matrix of PS [Fig. 4(b)]. This value is in good agreement with the theoretical one calculated on the basis of the tip-sample electrostatic interaction [24,25]: $\Delta x = (Rz_0)^{1/2} \sim 20$ nm. This result shows that PS and PVAc are immiscible at scale equal or lower than 30 nm. From the morphology image, we found a surface fraction of PVAc close to 14%, a value coherent with the polymer composition of the film. The direct confrontation of the topography with the dielectric map [Figs. 3(a) and 4(a)] points out that small satellite nodules (around 20 nm)

are detected in the dielectric map and not in the topography, thus showing the high sensitivity of this method.

In summary we have developed a reliable and accurate EFM-based method to quantitatively measure and image the dielectric constant of nanostructured complex system with unprecedented lateral resolution. This method is simple to implement on standard AFM setups and opens opportunities to study the dielectric properties in fields ranging from materials science to biology.

The financial support of Donostia International Physics Center (DIPC) is acknowledged. The authors would like to acknowledge the financial support provided by the Basque Country Government (Reference No. IT-436-07, Depto. Educación, Universidades e Investigación), the Spanish Ministry of Science and Innovation (Grant No. MAT 2007-63681), the European Community (SOFTCOMP program), and the PPF Rhéologie et plasticité des matériaux mous hétérogènes 2007–2010 Contract No. 20071656.

-
- [1] G. Binnig, C. F. Quate, and C. Gerber, *Phys. Rev. Lett.* **56**, 930 (1986).
 - [2] G. M. Sacha, E. Sahagun, and J. J. Saenz, *J. Appl. Phys.* **101**, 024310 (2007).
 - [3] S. Belaidi, P. Girard, and G. Lévêque, *J. Appl. Phys.* **81**, 1023 (1997).
 - [4] A. V. Krayev and R. V. Talroze, *Polymer* **45**, 8195 (2004).
 - [5] A. V. Krayev, G. A. Shandryuk, L. N. Grigorov, and R. V. Talroze, *Macromol. Chem. Phys.* **207**, 966 (2006).
 - [6] L. Fumagalli, G. Ferrari, M. Sampietro, and G. Gomila, *Nano Lett.* **9**, 1604 (2009).
 - [7] L. Fumagalli, G. Ferrari, M. Sampietro, and G. Gomila, *Appl. Phys. Lett.* **91**, 243110 (2007).
 - [8] L. Fumagalli, G. Ferrari, M. Sampietro, I. Casuso, E. Martinez, J. Samitier, and G. Gomila, *Nanotechnology* **17**, 4581 (2006).
 - [9] G. Gomila, J. Toset, and L. Fumagalli, *J. Appl. Phys.* **104**, 024315 (2008).
 - [10] W. Lu, D. Wang, and L. Chen, *Nano Lett.* **7**, 2729 (2007).
 - [11] G. Gramse, I. Casuso, J. Toset, L. Fumagalli, and G. Gomila, *Nanotechnology* **20**, 395702 (2009).
 - [12] P. S. Crider, M. R. Majewski, J. Zhang, H. Oukris, and N. E. Israeloff, *Appl. Phys. Lett.* **91**, 013102 (2007).
 - [13] P. S. Crider, M. R. Majewski, J. Zhang, H. Oukris, and N. E. Israeloff, *J. Chem. Phys.* **128**, 044908 (2008).
 - [14] L. Portes, P. Girard, R. Arinero, and M. Ramonda, *Rev. Sci. Instrum.* **77**, 096101 (2006).
 - [15] P. Girard, M. Ramonda, and D. Saluel, *J. Vac. Sci. Technol. B* **20**, 1348 (2002).
 - [16] L. Portes, M. Ramonda, R. Arinero, and P. Girard, *Ultramicroscopy* **107**, 1027 (2007).
 - [17] C. Riedel, R. Arinero, Ph. Tordjeman, M. Ramonda, G. Lévêque, G. A. Schwartz, D. Garcia de Oteyza, A. Alegria, and J. Colmenero, *J. Appl. Phys.* **106**, 024315 (2009).
 - [18] D. Hall, P. Underhill, and J. M. Torkelson, *Polym. Eng. Sci.* **38**, 2039 (1998).
 - [19] N. G. McCrum, B. E. Read, and G. Williams, *Anelastic and Dielectric Effects in Polymeric Solids* (Dover, New York, 1991).
 - [20] J. M. O'Reilly, *J. Polym. Sci.* **57**, 429 (1962).
 - [21] O. Yano and Y. Wada, *J. Polym. Sci., Part A-2* **9**, 669 (1971).
 - [22] G. A. Schwartz, J. Colmenero, and A. Alegria, *Macromolecules* **39**, 3931 (2006).
 - [23] L. Hutter and J. Bechhoefer, *Rev. Sci. Instrum.* **64**, 1868 (1993).
 - [24] S. Gomez-Monivas, L. S. Froufe, R. Carminati, J. J. Greffet, and J. J. Saenz, *Nanotechnology* **12**, 496 (2001).
 - [25] B. Bhushan and H. Fuchs, *Applied Scanning Probe Methods II* (Springer, New York, 2003), p. 312.